Turbulence in the Solar Corona

Steven R. Cranmer

Harvard-Smithsonian Center for Astrophysics, 60 Garden Street, Cambridge, MA 02138, USA

Abstract. The solar corona has been revealed in the past decade to be a highly dynamic nonequilibrium plasma environment. Both the loop-filled coronal base and the extended acceleration region of the solar wind appear to be strongly turbulent, but direct observational evidence for a cascade of fluctuation energy from large to small scales is lacking. In this paper I will review the observations of wavelike motions in the corona over a wide range of scales, as well as the macroscopic effects of wave-particle interactions such as preferential ion heating. I will also present a summary of recent theoretical modeling efforts that seem to explain the time-steady properties of the corona (and the fast and slow solar wind) in terms of an anisotropic MHD cascade driven by the partial reflection of low-frequency Alfvén waves propagating along the superradially expanding solar magnetic field. Complete theoretical models are difficult to construct, though, because many of the proposed physical processes act on a multiplicity of spatial scales (from centimeters to solar radii) with feedback effects not yet well understood. This paper is thus a progress report on various attempts to couple these disparate scales.

Keywords: solar corona, solar wind, MHD turbulence, Alfvén waves
PACS: 52.35.Bj, 52.35.Mw, 52.35.Ra, 95.55.Fw, 96.50.Ci, 96.50.Tf, 96.60.P-

INTRODUCTION

Astronomers often define "turbulence" rather loosely, as either a collection of motions that are unresolved either spatially or temporally, or as dynamical oscillations that exhibit a broad-band spectrum of frequencies and no clear dominant frequency. Our knowledge about turbulence in the solar corona comes mainly from observations of this kind. Iron-clad evidence for the existence of a turbulent cascade in the corona awaits *in situ* exploration such as a "Solar Probe" could provide [32]. Substantial progress has been made, though, on the basis of remote-sensing observations, extrapolation inward from existing *in situ* measurements, and theoretical modeling. This paper summarizes a cross section of these recent efforts to better understand the role of turbulence in the corona.

OBSERVATIONAL EVIDENCE

The turbulent solar photosphere is the natural lower boundary condition for fluctuations higher in the atmosphere [37]. The photosphere displays a superposition of both quasi-laminar granulation (i.e., overturning convective cells) and smaller-scale stochastic motions in the dark intergranular lanes. The latter are also associated with 100 km sized concentrations of magnetic field ($\sim$1.5 kG)—known as G-band bright points or magnetic bright points—that are shaken transversely by the granulation and appear to contain enough energy to give rise to coronal Alfvén waves [7].

Higher in the corona, plasma fluctuations reveal themselves by presenting variations in density, velocity, and magnetic field strength. These remotely measured quantities are most sensitive to the wave modes that carry the most energy, which are generally dominated by the longest wavelengths. Thus, *direct* measurements are typically interpreted as ideal MHD fluctuations. (Some indirect measurements provide constraints on small-scale kinetic modes; see below.) The major detection techniques are listed here:

1. **Intensity modulations** mainly probe variations in density, with the observed fluctuations being proportional to either ρ or ρ^2 (integrated along the line-of-sight) depending on the spectral band or lines used. Intensity oscillations measured with various instruments aboard the *Solar and Heliospheric Observatory* (*SOHO*) have implied the presence of compressive MHD waves channeled along magnetic flux tubes in coronal holes [9, 34].

2. **Motion tracking** in sequences of images can provide information about velocity fluctuations in the "plane of the sky" (i.e., the plane perpendicular to the line-of-sight direction). Cross-correlation techniques have been used to obtain the bulk solar wind acceleration of low-contrast "blobs" [42]. Recently, wavelet-enhanced [41] images and movies from the EIT and LASCO instruments on *SOHO* have enabled the filtering of fine-scale variations that were previously "hidden" in diffuse larger-scale coronal features.

3. **Doppler shifts** generally allow velocities along the line-of-sight direction to be probed. Time-resolved sinusoidal oscillations have been seen in some coronal structures [46, 35]. Most often, though, waves that reach into the solar wind are diagnosed via "Doppler broadening" of spectral lines that arises because of averaging over the oscillating redshifts and blueshifts. In the low corona, where all plasma species are expected to be collisionally coupled (and have identical temperatures), it is relatively straightforward to extract the "nonthermal" wave broadening from the thermal motions that also contribute to emission line widths. In the collisionless extended corona, though, there appears to be at least a mild decoupling between T_e and T_p as well as stronger preferential heating for heavy ions (see below). This complicates the analysis, but realistic limits can still be placed on transverse wave amplitudes [for summaries of existing data, see 5, 7, 14, 43].

4. **Radio sounding** probes the conditions in the corona by measuring distortions in the net refractive index of plasma that intervenes between a receiver and either a spacecraft beacon or a cosmic source (e.g., a pulsar or radio galaxy). These distortions are sensitive to density (from scintillations), velocity (from drifting diffraction patterns), and the magnetic field (from Faraday rotation). The wide range of spatial scales probed by radio diagnostics have allowed new constraints to be placed on the properties of turbulence in the corona [2, 4, 20, 22], but there is still something of a disconnect between the quantities that are measured directly and the quantities predicted by theory.

If the coronal fluctuations merely propagated upward on open field lines—without interacting with the background plasma—they would not be of much interest. Observations of how the plasma is heated and accelerated, presumably by *wave-particle interactions* in the collisionless outer corona, are useful as an indirect means of determining

which wave modes are generated and damped. The Ultraviolet Coronagraph Spectrometer (UVCS) on *SOHO* measured extremely high temperatures of heavy ions, faster ion outflow compared to protons, and strong anisotropies (in the sense $T_\perp > T_\parallel$) for ion velocity distributions in the extended corona [25, 26, 27]. These properties are shared by high-speed solar wind streams measured *in situ* [e.g., 30].

The UVCS observations have led to a resurgence of interest in ion cyclotron resonance as a likely mechanism for producing this kind of preferential ion energization, and possibly also for heating the bulk plasma as well [4, 22, 27]. Alfvén waves that are ion cyclotron resonant in the corona have frequencies in the 10^2–10^4 Hz range, whereas the measured and inferred frequencies are much smaller; 10^{-5}–10^{-2} Hz. Thus, *turbulent cascade* has long been considered a natural way to produce power at high frequencies from waves initially at lower frequencies. It is well known, though, that both numerical simulations and analytic descriptions of MHD turbulence (with a strong background "guide field" like in the corona) indicate that the cascade from small to large wavenumber occurs most efficiently for modes that do not increase in frequency (i.e., primarily a fast cascade in $k_\perp$ and negligible transport in $k_\parallel \sim \omega/V_A$). In the low-$\beta$ corona, this type of quasi-two-dimensional cascade would lead to kinetic Alfvén waves and preferential *electron* heating (in $T_\parallel$), which is not observed. This issue remains a topic of active research, with several possible outcomes depending on the behavior of the anisotropic cascade when kinetic processes become important [3, 6, 22, 29, 24, 39].

CORONAL HEATING AND SOLAR WIND ACCELERATION

Much of the above work dealt with determining the properties of the "microscopic" fluctuations that dissipate to heat the particles in the corona. Complementary progress has been made in constraining the "macroscopic" properties of the MHD turbulence that should eventually cascade down to the microscopic kinetic scales. In fact, if the precise distribution of energy into various channels (i.e., $T_e \neq T_p$ and $T_\parallel \neq T_\perp$) is ignored, it can be argued that the macroscopic level is all that is needed to compute how much energy will eventually be dissipated. This approach has been taken in recent models of turbulent heating of both closed loops in the low corona [38] and open flux tubes that reach into the solar wind [7, 8, 45].

The remainder of this paper presents results from a self-consistent treatment of coronal heating and solar wind acceleration that used a phenomenological description of imbalanced MHD turbulence [8]. The only input parameters to these models were the photospheric lower boundary conditions for the wave spectra and the radial dependence of the background magnetic field along the flux tube. The models are the first self-consistent solutions that combine: (a) chromospheric heating driven by an empirically guided acoustic wave/shock spectrum, (b) coronal heating from Alfvén waves that have been partially reflected, then damped via a turbulent cascade, and (c) solar wind acceleration from gradients of gas pressure, acoustic wave pressure, and Alfvén wave pressure.

The majority of heating in these models comes from the turbulent dissipation of partially reflected Alfvén waves [see also 31, 11, 45]. Measurements of G-band bright points in the photosphere were used to specify the Alfvén wave power spectrum at the lower boundary. Non-WKB wave transport equations were then solved to determine the

degree of linear reflection due to radial gradients in the background plasma parameters (mainly the Alfvén speed V_A). The resulting values of the Elsasser amplitudes $Z_\pm$, which denote the energy contained by upward (Z_-) and downward (Z_+) propagating waves, were then used to constrain the energy flux in the cascade. We used a phenomenological form for the nonlinear transport that has evolved from studies of reduced MHD and comparisons with numerical simulations. The adopted volumetric heating rate (erg s^{-1} cm^{-3}) is given by

$$Q_A = \rho \left(\frac{1}{1 + [t_{\mathrm{eddy}}/t_{\mathrm{ref}}]^n} \right) \frac{Z_-^2 Z_+ + Z_+^2 Z_-}{4L_\perp} \tag{1}$$

[e.g., 23, 50, 11, 8]. The transverse length scale $L_\perp$ represents an effective perpendicular correlation length of the turbulence, and we used the standard assumption that $L_\perp$ scales with the cross-sectional width of the flux tube [21]. The term in parentheses above is an efficiency factor that accounts for situations when the cascade does not have time to develop before the waves or the wind carry away the energy [10]. The classical Kolmogorov-like cascade is thus "quenched" when the nonlinear eddy time scale t_{eddy} becomes much longer than the macroscopic wave reflection time scale t_{ref}. In most of the models we used $n = 1$ based on analytic and numerical models [12, 36], but we also tried $n = 2$ to explore a stronger form of this quenching.

Figure 1 summarizes the results of varying the magnetic field properties while keeping the lower boundary conditions fixed [8]. The models included polar coronal holes, equatorial streamers (as well as the full latitudinal variation between the two at solar minimum) and open flux tubes rooted in active regions. We found that a realistic variation of asymptotic solar wind conditions can be produced by varying only the background magnetic field geometry, as predicted by Wang and Sheeley [47, 48, 49]. Specifically, the models show general agreement with some well known empirical correlations: i.e., a larger coronal expansion factor gives rise to a slower and denser wind, less intense Alfvénic fluctuations at 1 AU, and larger values of both the O^{7+}/O^{6+} charge state ratio and the FIP-sensitive Fe/O abundance ratio. Satisfying these kinds of observational scalings are necessary but not sufficient conditions for validating the idea that the solar wind is driven by a combination of MHD turbulence and non-WKB Alfvén wave reflection.

The models shown in Figure 1 are limited by being one-dimensional, time-independent, and one-fluid descriptions of a plasma that, in reality, is none of those things. Future work must involve including the divergent temperatures and flow speeds of protons, electrons, and various heavy ion species in the extended corona and heliosphere. Even simple two-fluid effects ($T_e \neq T_p$) can affect the macroscopic distribution of heat flux [19], the dynamical stability of closed-field regions like streamers [13], and possibly even the phenomenological form of the MHD turbulent cascade [16]. Also, the inclusion of compressive MHD modes may also affect many important properties of the anisotropic cascade [e.g., 3].

It is also likely that in certain regions of the corona, waves and turbulence (by themselves) cannot be the whole story. For example, it seems increasingly clear that the bright coronal loops seen in UV and X-ray images are heated by some variety of intermittent magnetic reconnection. The question remains whether such a collection of bursty heating events is powered mainly by: (a) direct stressing of the magnetic
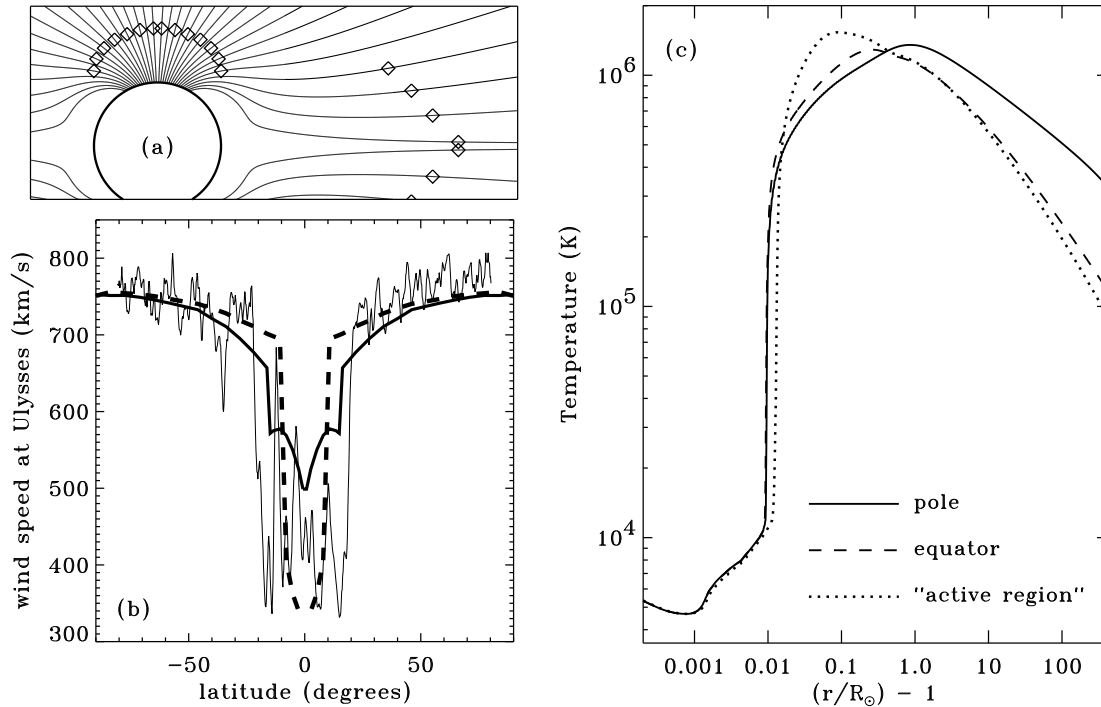
FIGURE 1. Summary of recent turbulence-driven coronal heating and solar wind acceleration models. **(a)** Adopted magnetic field geometry [1], with radii of wave-modified critical points marked by open diamonds. **(b)** Latitudinal dependence of outflow speed at ∼2 AU for models with $n = 1$ (thick solid curve) and $n = 2$ (dashed curve), compared with data from the *Ulysses* polar pass in 1994–1995 (thin solid curve) [17]. **(c)** Radial temperature dependence of polar coronal hole model (solid curve), equatorial streamer-edge model (dashed curve), and strong-field active region model (dotted curve). Additional details about these models can be found in [8].

footpoints [e.g., 18], (b) newly emerging magnetic flux from below the photosphere [15, 40], (c) long-time buildup of non-potential shear [28], or (d) some combination of the above ideas. It is possible that concepts from turbulence theory may be applicable to these kinds of processes as well [44, 33].

ACKNOWLEDGMENTS

REFERENCES

1. M. Banaszkiewicz, W. I. Axford, and J. F. McKenzie, *Astron. Astrophys.* **337**, 940 (1998).
2. T. S. Bastian, *Astrophys. Space Sci.* **277**, 107 (2001).
3. B. D. G. Chandran, *Phys. Rev. Lett.* **95**, 265004 (2005).
4. S. R. Cranmer, *Space Sci. Rev.* **101**, 229 (2002).

5. S. R. Cranmer, "Observational Aspects of Wave Acceleration in Open Magnetic Regions," in *SOHO-13: Waves, Oscillations, and Small-scale Events in the Solar Atmosphere,* edited by H. Lacoste, ESA SP-547, ESA, Noordwijk, 2004, p. 353 (astro-ph/0309676).
6. S. R. Cranmer, and A. A. van Ballegooijen, *Ap. J.* **594**, 573 (2003).
7. S. R. Cranmer, and A. A. van Ballegooijen, *Ap. J. Suppl.* **156**, 265 (2005).
8. S. R. Cranmer, A. A. van Ballegooijen, and R. J. Edgar, *Ap. J. Suppl.* **171**, in press, astro-ph/0703333 (2007).
9. C. E. DeForest, and J. B. Gurman, *Ap. J.* **501**, L217 (1998).
10. P. Dmitruk, and W. H. Matthaeus, *Ap. J.* **597**, 1097 (2003).
11. P. Dmitruk, W. H. Matthaeus, L. J. Milano, et al., *Ap. J.* **575**, 571 (2002).
12. M. Dobrowolny, A. Mangeney, and P. Veltri, *Phys. Rev. Lett.* **45**, 144 (1980).
13. E. Endeve, T. E. Holzer, and E. Leer, *Ap. J.* **603**, 307 (2004).
14. R. Esser, et al., *Ap. J.* **510**, L63 (1999).
15. L. A. Fisk, L. A. 2003, *J. Geophys. Res.* **108** (A4), 1157 (2003).
16. S. Galtier, *J. Plasma Phys.* **72**, 721 (2006).
17. B. E. Goldstein, et al., *Astron. Astrophys.* **316**, 296 (1996).
18. B. V. Gudiksen, "DC Heating: Is it Enough?" in *Solar Wind 11/SOHO–16: Connecting Sun and Heliosphere,* edited by B. Fleck, T. Zurbuchen, & H. Lacoste, ESA SP-592, ESA, Noordwijk, 2005, p. 165.
19. V. H. Hansteen, and E. Leer, *J. Geophys. Res.* **100**, 21577 (1995).
20. J. K. Harmon, and W. A. Coles, *J. Geophys. Res.* **110**, A03101 (2005).
21. J. V. Hollweg, *J. Geophys. Res.* **91**, 4111 (1986).
22. J. V. Hollweg, *Phil. Trans. Roy. Soc. A* **364**, 505 (2006).
23. M. Hossain, P. C. Gray, D. H. Pontius, Jr., et al., *Phys. Fluids* **7**, 2886 (1995).
24. G. G. Howes, S. C. Cowley, W. Dorland, et al., *Ap. J.* **651**, 590 (2006).
25. J. L. Kohl, et al., *Solar Phys.* **175**, 613 (1997).
26. J. L. Kohl, et al., *Ap. J.* **501**, L127 (1998).
27. J. L. Kohl, G. Noci, S. R. Cranmer, and J. C. Raymond, *Astron. Astrophys. Review* **13**, 31 (2006).
28. D. W. Longcope, "Quantifying Magnetic Reconnection and the Heat it Generates," in *SOHO-15: Coronal Heating,* edited by R. W. Walsh, J. Ireland, D. Danesy, & B. Fleck, ESA SP-575, ESA, Noordwijk, 2004, p. 198.
29. S. A. Markovskii, B. J. Vasquez, C. W. Smith, and J. V. Hollweg, *Ap. J.* **639**, 1177 (2006).
30. E. Marsch, *Space Sci. Rev.* **87**, 1 (1999).
31. W. H. Matthaeus, G. P. Zank, S. Oughton, D. J. Mullan, and P. Dmitruk, *Ap. J.* **523**, L93 (1999).
32. D. J. McComas, et al., *Rev. Geophys.* **45**, RG1004 (2007).
33. L. J. Milano, D. O. Gómez, and P. C. H. Martens, *Ap. J.* **490**, 442 (1997).
34. L. Ofman, M. Romoli, G. Poletto, G. Noci, and J. L. Kohl, *Ap. J.* **529**, 592 (2000).
35. E. O'Shea, D. Banerjee, and J. G. Doyle, *Astron. Astrophys.* **463**, 713 (2007).
36. S. Oughton, P. Dmitruk, and W. H. Matthaeus, *Phys. Plasmas* **13**, 042306 (2006).
37. K. Petrovay, *Space Sci. Rev.* **95**, 9 (2001).
38. A. F. Rappazzo, M. Velli, G. Einaudi, and R. B. Dahlburg, 2007, *Ap. J.* **657**, L47 (2007).
39. A. A. Schekochihin, S. C. Cowley, W. Dorland, et al., *Ap. J. Suppl.,* submitted, astro-ph/arXiv:0704.0044v1 (2007).
40. N. A. Schwadron, and D. J. McComas, *Ap. J.* **599**, 1395 (2003).
41. G. Stenborg, and P. J. Cobelli, *Astron. Astrophys.* **398**, 1185 (2003).
42. S. J. Tappin, G. M. Simnett, and M. A. Lyons, *Astron. Astrophys.* **350**, 302 (1999).
43. C.-Y. Tu, and E. Marsch, *Space Sci. Rev.* **73**, 1 (1995).
44. A. A. van Ballegooijen, *Ap. J.* **311**, 1001 (1986).
45. A. Verdini, and M. Velli, *Ap. J.* in press, astro-ph/0702205 (2007).
46. T. J. Wang, S. K. Solanki, W. Curdt, et al., *Astron. Astrophys.* **406**, 1105 (2003).
47. Y.-M. Wang, and N. R. Sheeley, Jr. *Ap. J.* **355**, 726 (1990).
48. Y.-M. Wang, and N. R. Sheeley, Jr. *Ap. J.* **372**, L45 (1991).
49. Y.-M. Wang, and N. R. Sheeley, Jr. *Ap. J.* **653**, 708 (2006).
50. Y. Zhou, and W. H. Matthaeus, *J. Geophys. Res.* **95**, 10291 (1990).